

Nucleic Acid Nanotechnology: Modified Backbones and Topological Polymer Templates 1
2

Philip Lukeman 3

Abstract DNA-based nanotechnology has revolutionized the construction of 4
nanoscale objects and devices—primarily by using Watson–Crick base-pairing to 5
program the self-assembly (and reaction pathways) of DNA oligomers into 6
branched structures. However, Watson–Crick-controlled self-assembly is not lim- 7
ited to the use of the “natural” D-(deoxy)ribose phosphodiester backbone. 8

This chapter describes nanoscale objects synthesized from oligomers containing 9
sugars other than D-deoxyribose or linkages other than phosphodiester linkages. 10
This chapter also focuses on using the backbone of DNA as a topological guide for 11
polymer synthesis. 12

As these chemical modifications profoundly affect the bioavailability, nuclease 13
resistance, protein binding, optoelectronic, and materials properties of nano-objects 14
compared to their “natural” DNA counterparts, they may find great utility in 15
biomedicine. 16

Keywords DNA • Polynucleotides • Templated syntheses • Backbones • Nylon • 17
Conducting polymers • Nanotechnology • DNA nanotechnology • DNA-based 18
nanotechnology • Junctions • L-DNA • PNA • LNA • GNA • Methylphosphonate 19

Contents 20

1	Introduction	00	21
2	Unusual Oligonucleotide Backbones in Junction-Based Nanosystems	00	22
	2.1 Future Directions for Unusual Oligonucleotide Backbones	00	23

P. Lukeman (✉)
Chemistry Department, St. John’s University, 8000 Utopia Parkway, St Albert’s Hall, Queens,
NY 11439, USA
e-mail: lukemanp@stjohns.edu

24	3	Topological Polymer Synthesis Using the DNA Backbone	00
25	3.1	Future Directions for Topological Polymer Synthesis	00
26	4	Summary	00
27		References	00

28 **1 Introduction**

29 This chapter is aimed at summarizing recent research diversifying the backbone of
 30 polynucleotides used in DNA-based nanoconstructions and using the backbone of
 31 DNA to control polymer synthesis (Fig. 1).

32 DNA-based nanotechnology has been influenced by many approaches, branched
 33 into many disciplines, and spawned many applications. By necessity, the vast
 34 majority of these streams, while *related* to the title of this chapter, are not described.
 35 Below are a series of leading references for the interested reader.

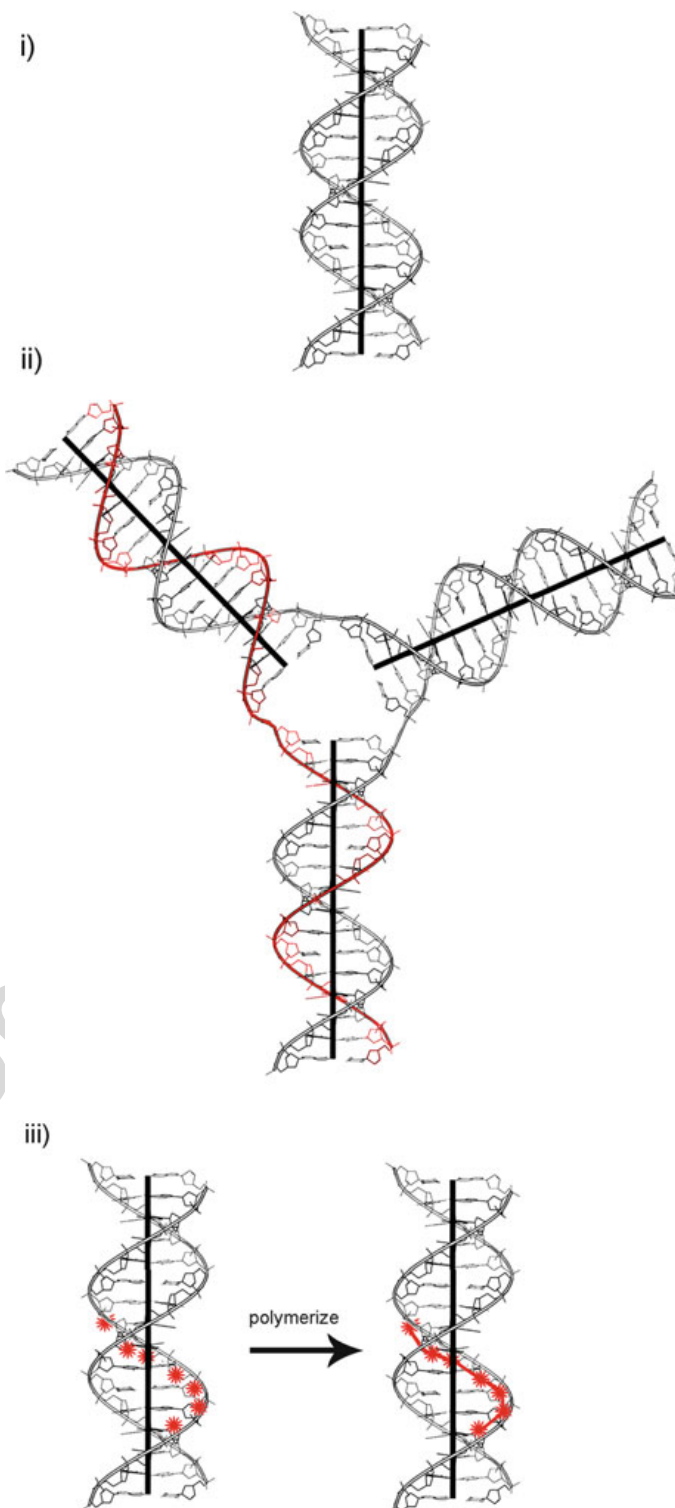
36 While there is a vast literature on construction using nonlinear DNA, this chapter
 37 is not a general review (Seeman 2010; Pinheiro et al. 2011) of DNA-based
 38 nanotechnology (Seeman 1982), nor a general review (Sacca and Niemeyer 2012)
 39 of DNA origami (Rothemund 2006); the chapter is not a review of triplex-based
 40 nanostructures (Fox and Brown 2005; Mukherjee and Vasquez 2011) nor of
 41 dendrimer-based DNA nanostructures (Caminade et al. 2008), nor of knotted or
 42 otherwise topologically intertwined DNA structures (Dobrowolski 2003).

43 There are many modified oligonucleotides that have been synthesized for a
 44 variety of purposes. This chapter does not cover modified oligonucleotides for
 45 antisense applications (Yamamoto et al. 2011; Keum et al. 2011), nor alternative
 46 base-pairing in DNA (Wojciechowski and Leumann 2011) including metal base
 47 pairs (Clever and Shionoya 2010), nor click chemistry as applied to
 48 oligonucleotides (El-Sagheer and Brown 2010), nor azobenzene-based switching
 49 of DNA (Beharry and Woolley 2011). Defined, branched nanostructures have been
 50 constructed using metal–ligand interactions (Yang et al. 2010) and using DNA as
 51 “smart-glue” to hold together various nanoparticles (Geerts and Eiser 2010)—this
 52 chapter does not cover these either.

53 The covalent chemistry touched upon in this chapter has also been used for
 54 functionalizing DNA nanostructures with proteins (Sacca and Niemeyer 2011) and
 55 to template small-molecule synthesis for reaction discovery (Kleiner et al. 2011) and
 56 macrocycle production (Milnes et al. 2012). Generally, if the modification is merely
 57 at the 3' or 5' end of an oligonucleotide or duplex, this chapter will not cover it.

58 The backbone of DNA has been used as a template for semiconducting materials
 59 (Houlton et al. 2009) and dye/ π systems (Ruiz-Carretero et al. 2011). Duplexes of
 60 every flavor using many phosphodiester-backbone (Eschenmoser 2011) and
 61 peptide-backbone (Nielsen 2010)-based structures have been synthesized; base-
 62 pairing has been used to template the synthesis of unnatural polymers (Brudno and
 63 Liu 2009); again, these topics are not the subject of this chapter.

Fig. 1 (i) A diagram showing a B-DNA double helix. Note the “helix axis”—a *central line* proceeding down the double helix. The duplex structures described in the chapter are predominantly B-like. (ii) The first part of this chapter describes modifications to the backbone of DNA (the internucleotide linkage and sugar-modified parts are highlighted in red) and these modified polynucleotides incorporation into branched structures (the example shown is a three-way “junction” where multiple helix axes converge). (iii) The second part of this chapter describes polynucleotides functionalized with reactive groups (schematically illustrated with *red stars*) that can react to form a polymer that follows the backbone of duplex DNA



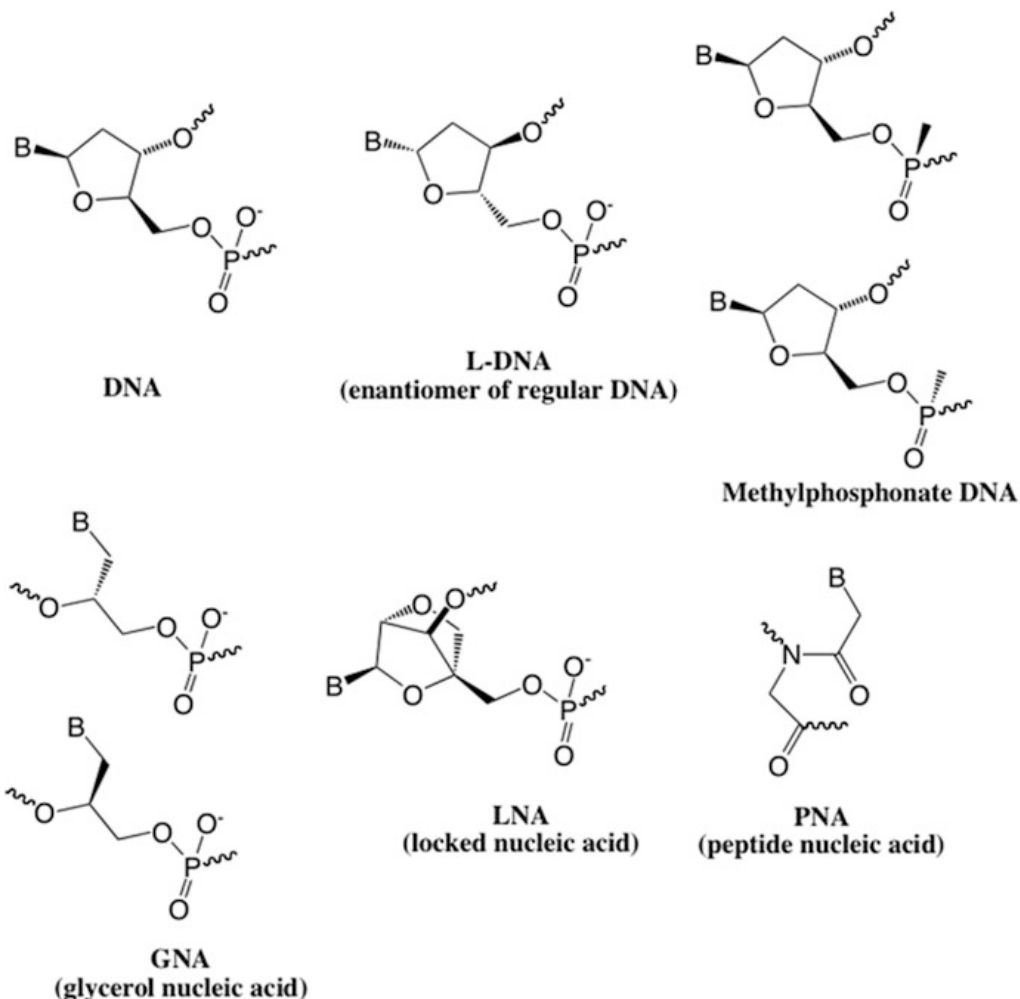


Fig. 2 The modified nucleotides referred to in this chapter

64 It is worth beginning this chapter by highlighting the chemical structure of the
 65 oligonucleotides used and thinking about the use of nonlinear DNA in
 66 nanoconstructions.

67 2 Unusual Oligonucleotide Backbones in Junction-Based 68 Nanosystems

69 Figure 2 shows the modified nucleotide backbones described in this chapter. As
 70 well as the commonalities of using the nucleobases A, T, G, and C to form
 71 Watson–Crick-paired structures, there are differences: there are 4-, 5-, and 6-
 72 atom repeats for the backbone, and both charged and uncharged structures. The
 73 ability of these diverse backbones to support duplex formation is utilized in the
 74 work that follows.

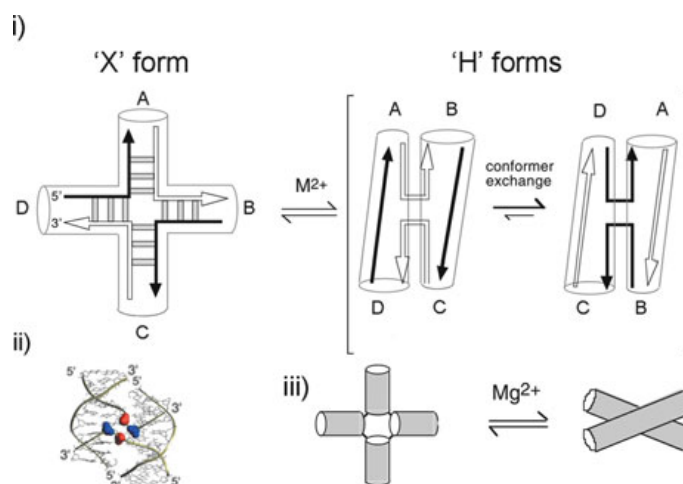


Fig. 3 (i) Schematic to illustrate the ion-induced folding of the four-way DNA junction into two possible stacked conformers. The junction comprises four DNA strands that associate to form the four helical arms A, B, C, and D. In the absence of added metal ions, the unmodified junction is extended into an “X” conformation, with the four arms directed toward the corners of a *square* shown on the *left*. On addition of metal ions, the junction may undergo a transition to form the stacked “H”-structure by pairwise coaxial stacking of helical arms. This can exist in either of two conformers—with the ratio of conformers being predominantly controlled by sequence of nucleotides at the junction. The junctions used in this chapter have sequences whose equilibria are biased toward the rightmost conformation, or are otherwise constrained. (ii) An illustration showing the proximity of phosphate groups in the stacked junction conformation. (iii) A simplified version of the Mg^{2+} -dependent equilibrium. Image used with permission (Liu et al. 2004)

As with other macromolecules, in order to use DNA for construction on the nanoscale the researcher requires an understanding of primary through quaternary structure. DNA Junctions, which can be thought of as points at which three or more helical axes converge, are the key secondary structure element required to make nonlinear objects, lattices, and devices from polynucleotides (Seeman 2010).

The archetypal (Kallenbach et al. 1983) four-way junction used in DNA nanotechnology has two gross conformational populations (Duckett et al. 1988); an extended “X” like conformation in which the four helical domains are unstacked, and stacked “H” like structures in which pairs of helical domains stack on top of each other (Fig. 3). The equilibrium between these conformations is sensitive to metal ion concentration; maximizing the energetically favorable base stacking in the H form involves the juxtaposition of phosphates that repel each other.

A four-way junction was investigated using methylphosphonate substitution (Liu et al. 2004) to address charge-related issues. This study demonstrated that the nature of the central phosphate groups of the “exchanging” strands were crucial to the metal ion determined stability of the junction. If both phosphates were substituted with methylphosphonate groups, the junction folded into the “H” conformation without addition of metal ions. Replacement of a single phosphate group reduced the requirement for metal ions in folding; the phosphate groups in proximity to the junction also exerted a significant influence on the folding process. The effect is subtle; further study (Liu et al. 2005) using diastereopure

96 methylphosphonate substitution showed that metal ion coordination at the junction
97 is geometrically demanding (i.e., dependant on the orientation of the phosphate)
98 and not merely a regional charge screening effect.

99 What does this study have to do with DNA-based nanotechnology? The confor-
100 mation of a junction can be fixed in place by torsionally linking at least two
101 duplexes with at least one other junction. This is the technique used for
102 multijunction structures such as DX and nX tiles, triangles, and most origami
103 approaches. Interphosphate repulsion at these junctions still likely destabilizes
104 these structures in the absence of divalent metal ions. Repulsion-based destabili-
105 zation allows the formation of multimers and other undesirable nondesigned
106 structures at equilibrium in junction-based systems (Li et al. 1996); also, in dynamic
107 nucleic acid systems with strand displacement events (Zhang and Seelig 2011), new
108 equilibrium distributions can be established even from homogenous samples of
109 well-folded structures. The incorporation of uncharged nucleic acid analogues into
110 junction-based structures should allow the synthesis of robust structures with less
111 dependence on metal ion concentration, and less tendency to want to “relax” into
112 alternate, unwanted configurations.

113 A stereochemical study of four-way junctions was conducted with enantiomeric
114 L-DNA and DNA (Lin et al. 2009). Unsurprisingly, the junctions had identical
115 physical properties such as stability and gel mobility, and the expected mirror-
116 image CD spectra. However, their interaction with chiral reagents provides poten-
117 tial biological utility—the L-DNA junction was completely resistant to degradation
118 by exonuclease. As L-DNA has the same physical properties as DNA, the hard-won
119 design lessons of nucleic acid objects (providing they do not rely on
120 enantioselective interactions with the nanostructure) should be *directly* portable
121 to this polynucleotide.

122 Junctions were also synthesized from enantiomeric (R) and (S) GNA
123 oligonucleotides (Zhang et al. 2008). These materials again displayed identical
124 physical properties and mirror image CD spectra. However, the GNA junctions
125 had unusually high thermal stabilities—35 °C greater than the cognate DNA system;
126 this is a remarkable stability for a system formed bringing together polyanionic
127 species. As GNA does not pair with DNA, and the geometric parameters of the helix
128 are unknown, if this oligonucleotide is to be used in nanoconstructions significant
129 further study will be required. It is particularly tantalizing that such stable structures
130 are accessible via routine, commercial phosphoramidite chemistry that allows facile
131 synthesis of GNA–DNA chimeras; this is much simpler (and potentially
132 multiplexable) chemistry than, for example, synthesizing PNA–DNA hybrids.

133 Other structural considerations are necessary for the incorporation of nonnatural
134 polynucleotides into nanostructures. The DX tile (Li et al. 1996) was the first rigid,
135 well-defined, B-DNA nucleic acid motif that was capable of tiling the plane with
136 two-dimensional, sticky-end associated crystals (Winfree et al. 1998). It thus served
137 as an attractive target for the incorporation of modified polynucleotides.

138 A two-tile system was synthesized using uncharged PNA strands as one cross-
139 over strand per junction (Lukeman et al. 2004) in the DX tiles (Fig. 4). This system
140 showed reduced dependence on divalent ions; 50-mM sodium with no divalent

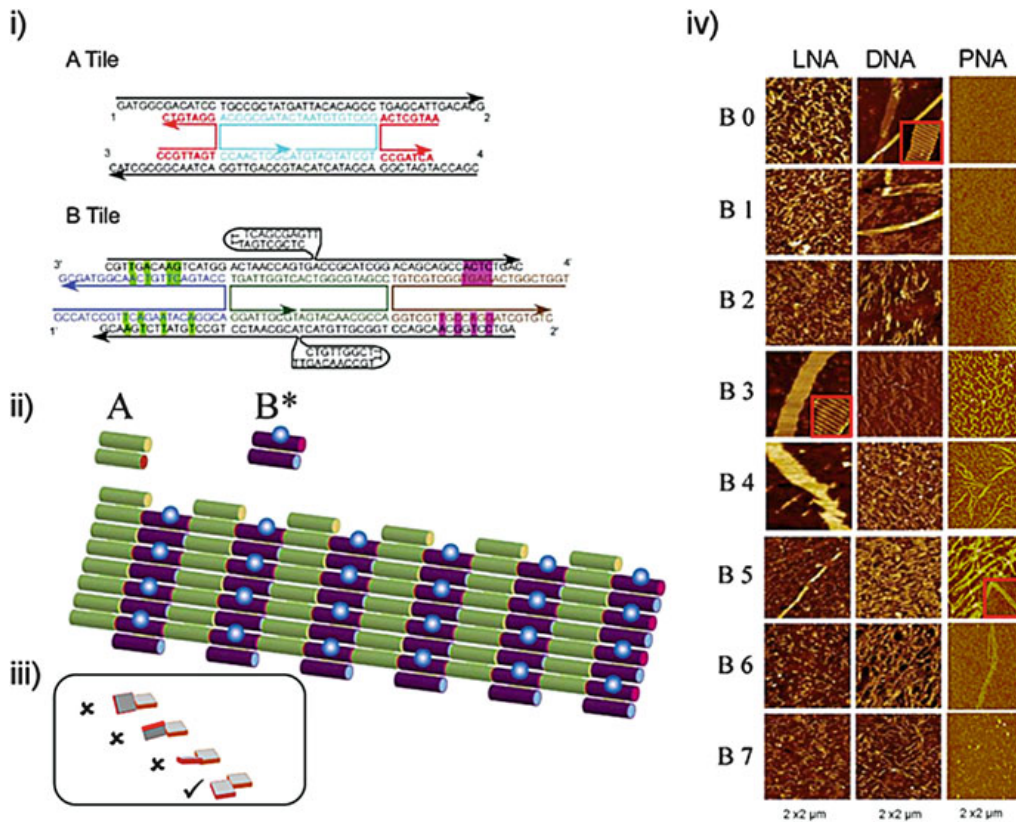


Fig. 4 (i) DX tiles used in this study. The *upper tile* is the A tile: the *red strands* are either LNA, PNA, or DNA. The *lower tile* is a version of the B tile. Base pairs are added alternately to the *left and right pairs* of outer arms to form tiles B1–B7 as shown by the *pink and green highlights*, e.g., to form B1 from B0, a base pair is added to both *pink regions*; to form B2 from B1, a base pair is added to both *green regions*. Complementary sticky ends are shown as numbers. All B tiles have hairpins, which will act as topographic markers when incorporated into an *array*. (ii) A and B* tiles forming a two-dimensional array. Helical regions are abstracted as *cylinders*, hairpins protruding from surface of array are abstracted as *dots*. (iii) PNA/LNA–DNA duplexes have a different helical repeat than DNA–DNA duplexes. Using the original “B0” design, the array will not form because the tiles are not held flat. In order to form flat arrays, we must alter geometry of other tile to compensate for this difference: adding bases to the “B” tile returns the system to planarity. The effect of adding extra bases to the B tile that bring the A tile back into the plane is shown here. (iv) AFM images of arrays formed from the tiles B0–B7. The images in the two columns are of a 2,000-nm field and the height scale is 6.0 nm. *Insets* for B3 (LNA), B0 (DNA), and B5 (PNA) show periodic features in well-formed arrays that correspond to different helical repeats of the duplex regions formed by the different polynucleotides. Images derived with permission (Rinker et al. 2006; Lukeman et al. 2004)

cation was sufficient to allow the tile to form at room temperature. Array synthesis 141
 failed using the system that worked for an all-DNA array; this was attributed to the 142
 difference in helical repeat of the PNA/DNA duplex that formed part of the tile. By 143
 systematically compensating for the changed helical repeat, arrays were formed 144
 successfully. This process also allowed the investigators to *measure* the helical 145
 repeat of the PNA/DNA duplex (15.6 bp/t with a maximum error of ± 1.4 bp/t 146
 measured over the 30 DNA–PNA base pairs present per tile) using picomole 147

148 quantities of sample. This helical repeat measuring technique appears to be general
149 for any polynucleotide that can form the outer arms of a DX. DX tiles capable of
150 forming two-dimensional arrays with LNA/DNA duplex arms were assembled
151 (Rinker et al. 2006), and the helical repeat was successfully measured (13.2 bp/t
152 with a maximum error of ± 0.9 bp/t).

153 Two-dimensional arrays and tubes were successfully constructed from single
154 strands of L-DNA (Lin et al. 2009); no compensation was needed for helical repeat
155 changes, as helical repeat is an achiral molecular property of the molecules.
156 However, AFM observation of this system nicely illustrated a microscopic to
157 macroscopic helical chirality transfer with enantiomeric strands forming “visibly”
158 enantiomeric micron-length tubes.

159 The assembly of hundreds of designed two-dimensional shapes from “Single
160 Stranded tiles” (Wei et al. 2012)—a kind of “scaffoldless” DNA origami—was
161 recently demonstrated. L-DNA was used to assemble ~ 15 nm \times 8 nm rectangular
162 system that was resistant to degradation by DNase I and T5 exonuclease.

163 2.1 *Future Directions for Unusual Oligonucleotide Backbones*

164 The menagerie (Eschenmoser 2011) of charged natural-nucleobase polynucleotides
165 used for investigation of origin-of-life studies and antisense purposes has not been
166 explored systematically for nanoconstruction; the two clear advantages of these
167 systems over regular DNA are thermal stability and nuclease resistance. Serum
168 survival times of nanoconstructions based on DNA appear to be significantly longer
169 (Mei et al. 2011; Walsh et al. 2011) than predicted (based on duplex stability), and
170 simple DNA-based nanomachines have been used in vivo to monitor (Bhatia et al.
171 2011; Surana et al. 2011) endocytotic processes; this implies, that at least for some
172 applications, modified nucleotide usage may not be necessary for in vivo work.

173 One selling point for these materials is the resultant assemblies’ thermal stabil-
174 ity; although covalent cross-linking (Rajendran et al. 2011; Tagawa et al. 2011) can
175 make assemblies far more stable to disassociation than any noncovalent approach.
176 These cross-linked assemblies are, however, covalently fixed, and, once so fixed,
177 are unable to undergo the branch-migration and strand-invasion driven processes
178 that complex folding pathways require.

179 Modified backbones can help with the above problem. Currently, complex DNA
180 systems with multiple helical regions have assembly kinetics that is programmed by
181 duplex length and GC content. Systems that have complex folding pathways are
182 designed to avoid kinetic-folding traps by having longer/GC heavier regions fold
183 first (Ke et al. 2012). There may be system designs where this process of optimizing
184 length and GC content are unfavorable for the structure’s formation. Using DNA *in*
185 *combination* with GNA or other polynucleotides capable of superstable base-
186 pairing as *structural elements* will allow the avoidance of assembly kinetic traps
187 while allowing the structure to be freed from length/GC content as a concern.

188 Uncharged polynucleotides have a broader range of uses; cell permeability and
189 trafficking, thermal stability, all forms of biomolecular interaction are all

profoundly affected by neutral or near-neutral species (in comparison to a polyanion like DNA). Unfortunately, even well-studied species like PNA exhibit serious conformational heterogeneity in a double-helical context (Totsingan et al. 2010), although this is being addressed by new derivatives (Corradini et al. 2011). The ability to play with charge to reliably modify biotransport properties of proteins is just now coming of age (Cronican et al. 2010); perhaps similar approaches can be used for nucleic acid assemblies.

3 Topological Polymer Synthesis Using the DNA Backbone

On one structural level, most of the structures described previously can be viewed as a series of “stick figures” (where each stick is the helix axis of DNA); these “sticks” are joined by junctions. At a finer level, the helical nature of DNA also allows one to control strand *topology*; the helical structure of the DNA backbone generates “nodes” (regions of lines crossing in space—the fundamental topological operator) (Seeman 2000); node control is the essence of synthesis of catenanes, catenates, and knots (Dobrowolski 2003). Due to sequence-level programmability and the large number of nodes that can be inserted into a DNA-based structure, there is no other molecular system that allows the construction of topological nanoscale objects with such fine control. For example, objects with braided topologies were generated using DNA and L-DNA as the source of positive and negative nodes (Ciengshin et al. 2011).

The backbones of these objects could act as *templates* for other polymer synthesis; other polymers have material properties that polynucleotides do not such as optical, electronic, or material strength.

Note that this approach is *not* the same as nucleating metal precipitation (Gu et al. 2006; Jones et al. 2011) or condensation of a polycation (Ma et al. 2004) on assembled DNA structures—this refers to a much finer angstrom-level control of individual covalent bonds “tracking” the helical path of a DNA strand.

The first controlled synthesis of a polymer following a DNA backbone was of the archetypal synthetic polymer—Nylon (Zhu et al. 2003). Modified deoxyuridine phosphoramidite monomers were synthesized with protected carboxylic acid and amine functionality appended to the 2' position of the ribose ring. These monomers are divided into two types: “polymer forming” and “cap forming.” The polymer-forming monomers were designed to display either a 5-carbon diamine (Unn) or a 5-carbon carboxylic acid (Ucc) upon deprotection; in the presence of condensing reagents, alternating Unn and Ucc monomers should form a “ladder polymer” along the backbone of the nucleic acid. The “cap forming” monomers displayed one amine (Un) or one carboxylic acid (Uc)—enabling the termination of polymer synthesis when positioned appropriately at the end of a polynucleotide sequence.

Poly-U segments displaying increasing numbers of amine/carboxylic acid functional groups were inserted into of a poly-T oligonucleotide; upon addition of a condensation reagent, up to four stereo-controlled amide bonds were formed up the

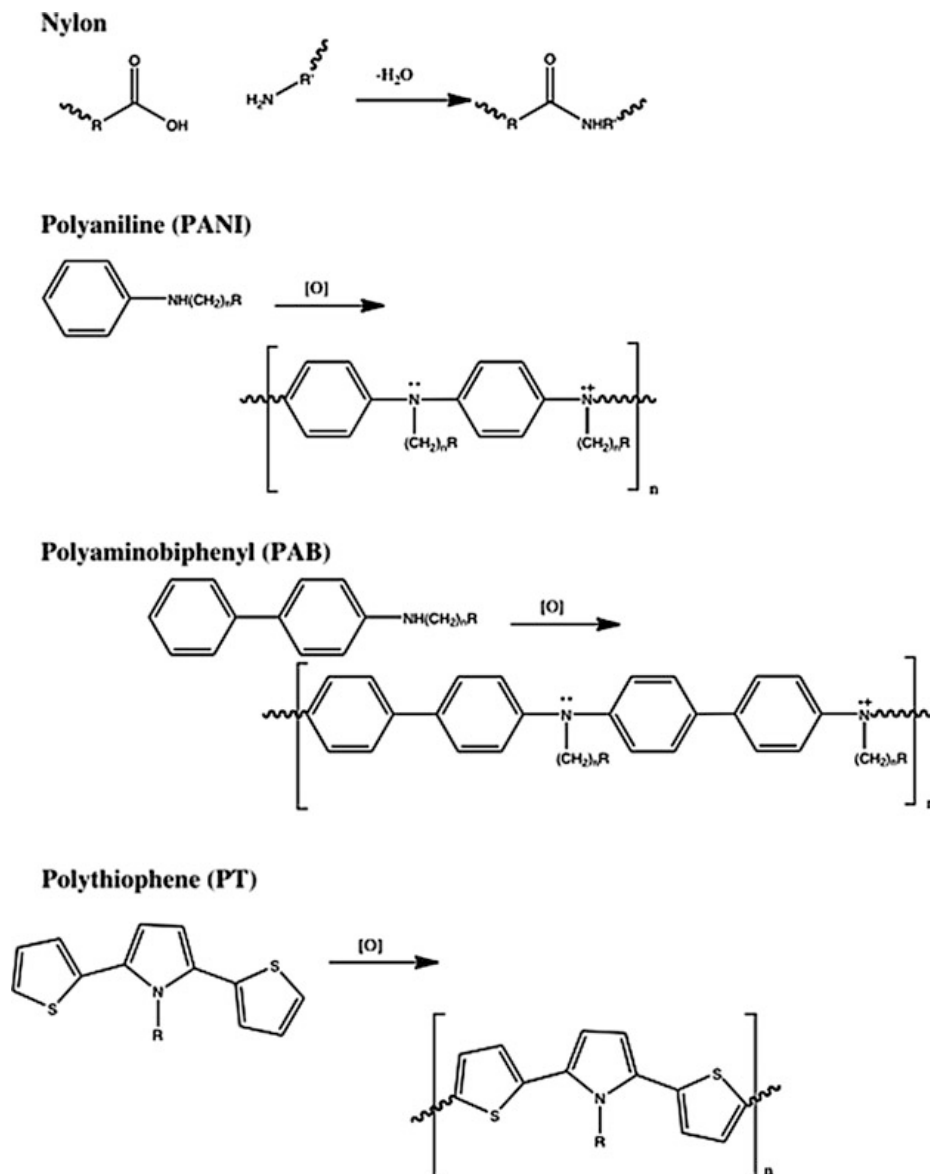


Fig. 5 The polymers referred to in this chapter

231 backbone of DNA. This synthesis was confirmed by gel electrophoresis and
 232 MALDI-MS with an estimated individual amide-bond forming yield of >95 %.

233 In follow-up work (Liu et al. 2008), the polymer synthesis was templated by
 234 hybridization to a complementary strand. This allowed for five amide bonds to be
 235 formed in higher yield and with greater ease of purification. Thermodynamic
 236 studies of these oligomers showed that both DNA and RNA duplexes formed
 237 from oligomers containing uncoupled side-groups were destabilized relative to
 238 their unmodified counterparts. The duplexes formed from coupled oligomer were,
 239 however, more stable than the uncoupled systems, and, with four or more amide
 240 bonds, coupled duplexes became more stable than the unmodified counterparts. As

estimated by Circular Dichroism, duplexes formed from coupled oligomer did not change gross conformation in comparison with their unmodified counterparts; thermodynamic study suggests that conformational preorganization of the ladder polymer plays a role in this increase in stability.

Further optimization (Liu et al. 2012) of the coupling and templation procedure (Fig. 6) allowed amide-bond formation yields to exceed 99 % and allowed the study of a molecule that contained seven amide bonds. Upon digestion with a nuclease, a neutral polynucleoside was formed where the oligomer was formed from the nylon backbone (via attachment to the 2' position on the sugar ring). Duplexes formed from this polynucleoside and DNA exhibited an unusual inverse stability dependence on salt concentration.

The DNA backbone has been used as a template for conducting polymer syntheses (Fig. 7). The convertible nucleotide approach allowed the attachment onto sequential nucleotides, of amines bearing aromatic rings capable of oxidative coupling. Upon hybridization to a complementary strand and oxidation, a templated polymer is formed. The first demonstration of this was with polyaniline (PANI) (Datta et al. 2006); up to six derivatized cytosines were placed in a duplex context and polymerized, with the polymer forming along the major groove according to modeling studies. The polymerization was duplex dependent; polymerization in the absence of partner formed branched product, which did not hybridize to its complement; UV spectra of untemplated reaction indicated less extended conjugation of the system.

In a follow-up study (Datta and Schuster 2008), longer stretches of PANI and 4'-aminobiphenyl (PAB) homopolymers (up to eight bases in sequence) were made, and the oxidation of these systems investigated; notable differences between the blue shift of increasingly conjugated PANI versus the geometry-restricted PAB were observed. Monomers that were blocked in the *para* position of the aromatic rings inhibited polymerization—along with UV spectra this confirms the presence of controlled PANI and PAB syntheses.

While the conjugation properties of these molecules was demonstrated with UV absorption spectra, the duplexes of both the unpolymerized and polymerized strands were destabilized relative to the unmodified system. The three-dimensional structure of PANI and PAB is incommensurate with that of DNA, limiting the length of polymer formation. In order to address the geometric incommensurability of PANI/PAB-based materials, polythiophene-like polymers (PT) using a duplex displaying alternating thymine and a thieno[3,2-b]pyrrole monomer were shown to oxidatively polymerize in a duplex context (Srinivasan and Schuster 2008), and still form B-DNA like products; however, stability of duplexes was still poor.

A more complete study was performed on 2,5-bis-(2-thienyl)pyrrole containing system (Chen et al. 2010), again showing complete polymerization, the expected UV properties of a conjugated system, CD properties of a B-like duplex. These duplexes were *stable* relative to duplex of the unmodified bases; indeed as the oligomers get longer, their stability in a duplex context increases relative to unmodified DNA. This monomer was used to make cyclic assemblies of up to 90 polymerized thiophene rings (Chen and Schuster 2012), the largest such stereocontrolled synthesis to date.

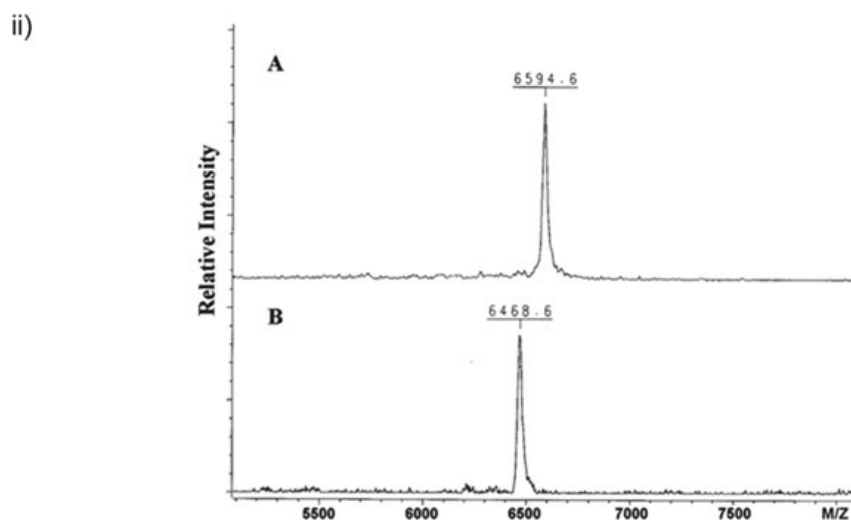
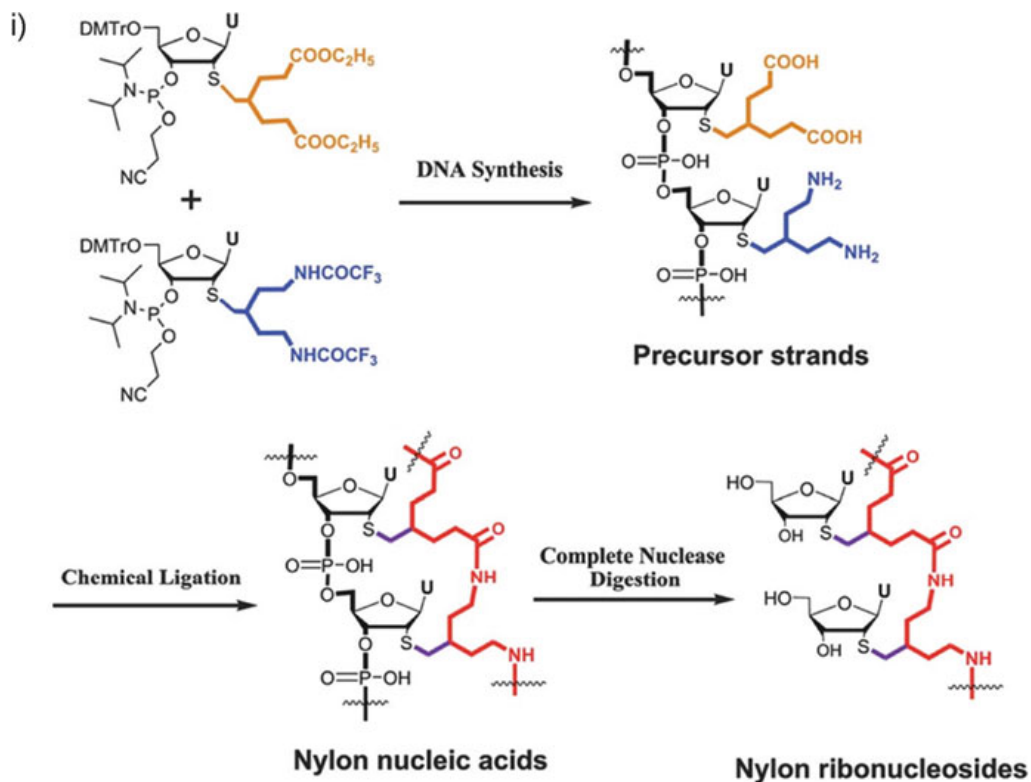
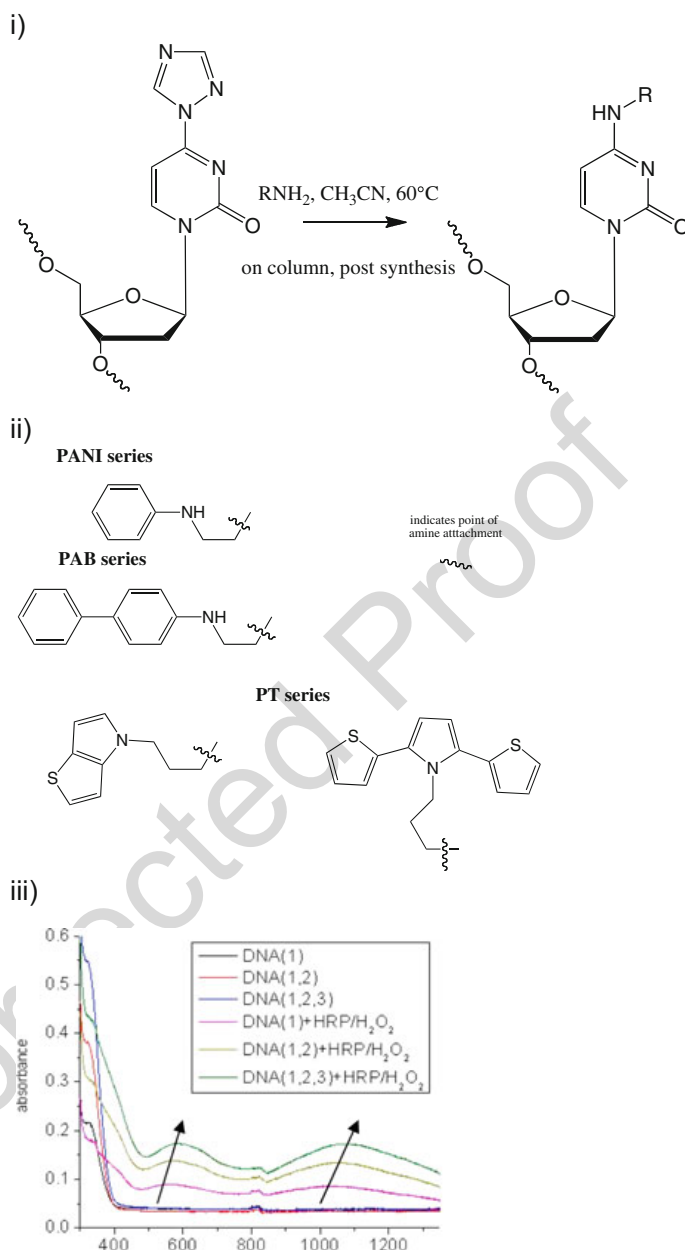


Fig. 6 (i) Nylon nucleic acid synthesis; monomers (*top left*), conventional DNA synthesis (*top right*), condensation/coupling using a dehydrating agent (*bottom left*) and complete nuclease digestion to produce nylon ribonucleotides (*bottom right*). (ii) MALDI-MS showing clean synthesis of a nylon nucleic acid from precursor containing eight contiguous monomers (*top spectrum* labeled A), clearly showing mass differential corresponding to a deficiency in seven water molecules (*bottom spectrum* labeled B). Image used with permission from Liu et al. (2012)

Fig. 7 (i) Oligomers displaying oxidizable aromatic rings can be synthesized using the convertible nucleotide approach. (ii) The oxidizable aromatic rings described in this chapter. (iii) UV-Vis-NIR absorption spectrum of DNA assemblies containing increasing lengths of PT monomers before and after reaction with HRP/H₂O₂. Before reaction with HRP/H₂O₂, all of DNA assemblies show absorptions that are the sum of those typical of the UV bands of DNA and the 320-nm band of these monomers. After reaction with HRP/H₂O₂, the absorption spectrum shifts revealing maxima at 560–580 nm and a band in the near IR region with a maximum at 1,030–1,070 nm. These spectral features are typical of the oxidized, conducting form of poly-2,5-bis (2-thienyl)-pyrrole



3.1 Future Directions for Topological Polymer Synthesis

286

The nylon-based chemistry described earlier is designed to be detached from the backbone via the liability of the carbon-sulfur linkage. Materials properties of catenanes and other topological objects constructed from a neutral polymer such as nylon will be open to investigation.

For the conducting polymer-based systems, if homogenous long conducting polymers can be generated, then signal transduction down these systems can be investigated using hole or electron injection as is done in conventional DNA

287

288

289

290

291

292

293

294 (Barton et al. 2011); new topologies should lead to a new understanding of
295 electronic properties at this scale. As DNA-based electrochemical signaling is
296 especially suited for detection in biofluids (Lubin and Plaxco 2010) (there are
297 very few electrochemically active contaminants in human sera, for example),
298 then applications involving, for example, fusions of aptamers with these conducting
299 polymers might provide a new sensing platform.

300 **4 Summary**

301 What about the future of the field? As stated above, modified backbones are just
302 beginning to be understood, and they are expensive compared to DNA. As one
303 colleague pointed out “we need to do a better, exhaustive job with the molecule that
304 we already understand and is dead cheap”; other chapters of this book describe such
305 approaches. This caution need not preclude sensible research into things that
306 generally cannot be done well with “vanilla” DNA, but like many “supramolecular”
307 fields, there is a certain sense of intellectual “territory-marking” that drives this
308 work.

309 Generally, the field of modified backbones “for and from” DNA nanotechnology
310 is a sack of solutions pleading for a problem—a “killer app,” to use terminology
311 from the software world. While some suggestions have been made above, the
312 scientific communities’ discernment and drive is the ultimate arbiter of whether
313 these assemblies move past their “curiosity” phase and live up to their evident
314 potential in biomedicine and beyond.

315 **References**

- 316 Barton JK, Olmon ED, Sontz PA (2011) Metal complexes for DNA-mediated charge transport.
317 *Coord Chem Rev* 255:619–634
- 318 Beharry AA, Woolley GA (2011) Azobenzene photoswitches for biomolecules. *Chem Soc Rev*
319 40:4422–4437
- 320 Bhatia D, Surana S, Chakraborty S et al (2011) A synthetic icosahedral DNA-based host-cargo
321 complex for functional in vivo imaging. *Nat Commun* 2:339
- 322 Brudno Y, Liu DR (2009) Recent progress toward the templated synthesis and directed evolution
323 of sequence-defined synthetic polymers. *Chem Biol* 16:265–276
- 324 Caminade AM, Turrin CO, Majoral JP (2008) Dendrimers and DNA: combinations of two special
325 topologies for nanomaterials and biology. *Chemistry* 14:7422–7432
- 326 Chen W, Schuster GB (2012) DNA-programmed modular assembly of cyclic and linear
327 nanoarrays for the synthesis of two-dimensional conducting polymers. *J Am Chem Soc*
328 134:840–843
- 329 Chen W, Guler G, Kuruvilla E et al (2010) Development of self-organizing, self-directing
330 molecular nanowires: synthesis and characterization of conjoined DNA-2,5-bis (2-thienyl)
331 pyrrole oligomers. *Macromolecules* 43:4032–4404
- 332 Ciengshin T, Sha R, Seeman NC (2011) Automatic molecular weaving prototyped by using single-
333 stranded DNA. *Angew Chem Int Ed* 50:4419–4422

Clever GH, Shionoya M (2010) Metal-base pairing in DNA. <i>Coord Chem Rev</i> 254:2391–2402	334
Corradini R, Sforza S, Tedeschi T et al (2011) Peptide nucleic acids with a structurally biased backbone. Updated review and emerging challenges. <i>Curr Top Med Chem</i> 11:1535–1554	335 336
Cronican JJ, Thompson DB, Beier KT et al (2010) Potent delivery of functional proteins into mammalian cells <i>in vitro</i> and <i>in vivo</i> using a supercharged protein. <i>ACS Chem Biol</i> 5:747–752	337 338
Datta B, Schuster GB (2008) DNA-directed synthesis of aniline and 4-aminobiphenyl, oligomers: programmed transfer of sequence information to a conjoined polymer nanowire. <i>J Am Chem Soc</i> 130:2965–2973	339 340 341
Datta B, Schuster GB, McCook A et al (2006) DNA-directed assembly of polyanilines: modified cytosine nucleotides transfer sequence programmability to a conjoined polymer. <i>J Am Chem Soc</i> 128:14428–14429	342 343 344
Dobrowolski JC (2003) DNA knots and links. <i>Polimery</i> 48:3–15	345
Duckett DR, Murchie AIH, Diekmann S et al (1988) The structure of the holliday junction, and its resolution. <i>Cell</i> 55:79–89	346 347
El-Sagheer AH, Brown T (2010) Click chemistry with DNA. <i>Chem Soc Rev</i> 39:1388–1405	348
Eschenmoser A (2011) Etiology of potentially primordial biomolecular structures: from vitamin B12 to the nucleic acids and an inquiry into the chemistry of life's origin: a retrospective. <i>Angew Chem Int Ed</i> 50:12412–12472	349 350 351
Fox KR, Brown T (2005) An extra dimension in nucleic acid sequence recognition. <i>Q Rev Biophys</i> 38:311–320	352 353
Geerts N, Eiser E (2010) DNA-functionalized colloids: physical properties and applications. <i>Soft Matter</i> 6:4647–4660	354 355
Gu Q, Cheng CD, Gonela R et al (2006) DNA nanowire fabrication. <i>Nanotechnology</i> 17:R14–R25	356
Houlton A, Pike AR, Galindo MA et al (2009) DNA-based routes to semiconducting nanomaterials. <i>Chem Commun</i> 14:1797–1806	357 358
Jones MR, Osberg KD, Macfarlane RJ et al (2011) Templated techniques for the synthesis and assembly of plasmonic nanostructures. <i>Chem Rev</i> 111:3736–3827	359 360
Kallenbach NR, Ma RI, Seeman NC (1983) An immobile nucleic-acid junction constructed from oligonucleotides. <i>Nature</i> 305:829–831	361 362
Ke Y, Bellot G, Voigt NV et al (2012) Two design strategies for enhancement of multilayer-DNA-origami folding: underwinding for specific intercalator rescue and staple-break positioning. <i>Chem Sci</i> 3:2587–2597	363 364 365
Keum JW, Ahn JH, Bermudez H (2011) Design, assembly, and activity of antisense DNA nanostructures. <i>Small</i> 7:3529–3535	366 367
Kleiner RE, Dumelin CE, Liu DR (2011) Small-molecule discovery from DNA-encoded chemical libraries. <i>Chem Soc Rev</i> 40:5707–5717	368 369
Li XJ, Yang XP, Qi J et al (1996) Antiparallel DNA double crossover molecules as components for nanoconstruction. <i>J Am Chem Soc</i> 118:6131–6140	370 371
Lin CX, Ke YG, Li Z et al (2009) Mirror image DNA nanostructures for chiral supramolecular assemblies. <i>Nano Lett</i> 9:433–436	372 373
Liu J, Declais AC, Lilley DMJ (2004) Electrostatic interactions and the folding of the four-way DNA junction: analysis by selective methyl phosphonate substitution. <i>J Mol Biol</i> 343:851–864	374 375
Liu J, Declais AC, McKinney SA et al (2005) Stereospecific effects determine the structure of a four-way DNA junction. <i>Chem Biol</i> 12:217–228	376 377
Liu Y, Wang RS, Ding L et al (2008) Thermodynamic analysis of nylon nucleic acids. <i>Chembiochem</i> 9:1641–1648	378 379
Liu Y, Wang R, Ding L et al (2012) Templated synthesis of nylon nucleic acids and characterization by nuclease digestion. <i>Chem Sci</i> 3:1930–1937	380 381
Lubin AA, Plaxco KW (2010) Folding-based electrochemical biosensors: the case for responsive nucleic acid architectures. <i>Acc Chem Res</i> 43:496–505	382 383
Lukeman PS, Mittal AC, Seeman NC (2004) Two dimensional PNA/DNA arrays: estimating the helicity of unusual nucleic acid polymers. <i>Chem Commun (Camb)</i> 15:1694–1695	384 385
Ma Y, Zhang J, Zhang G et al (2004) Polyaniline nanowires on si surfaces fabricated with DNA templates. <i>J Am Chem Soc</i> 126:7097–7101	386 387

- 388 Mei QA, Wei XX, Su FY et al (2011) Stability of DNA origami nanoarrays in cell lysate. *Nano*
389 *Lett* 11:1477–1482
- 390 Milnes PJ, McKee ML, Bath J et al (2012) Sequence-specific synthesis of macromolecules using
391 DNA-templated chemistry. *Chem Commun* 48:5614–5616
- 392 Mukherjee A, Vasquez KM (2011) Triplex technology in studies of DNA damage, DNA repair,
393 and mutagenesis. *Biochimie* 93:1197–1208
- 394 Nielsen PE (2010) Peptide nucleic acids (PNA) in chemical biology and drug discovery. *Chem*
395 *Biodivers* 7:786–804
- 396 Pinheiro AV, Han DR, Shih WM et al (2011) Challenges and opportunities for structural DNA
397 nanotechnology. *Nat Nanotechnol* 6:763–772
- 398 Rajendran A, Endo M, Katsuda Y et al (2011) Photo-cross-linking-assisted thermal stability of
399 DNA origami structures and its application for higher-temperature self-assembly. *J Am Chem*
400 *Soc* 133:14488–14491
- 401 Rinker S, Liu Y, Yan H (2006) Two-dimensional LNA/DNA arrays: estimating the helicity of
402 LNA/DNA hybrid duplex. *Chem Commun* 25:2675–2677
- 403 Rothemund PWK (2006) Folding DNA to create nanoscale shapes and patterns. *Nature*
404 440:297–302
- 405 Ruiz-Carretero A, Janssen PGA, Kaeser A et al (2011) DNA-templated assembly of dyes and
406 extended pi-conjugated systems. *Chem Commun* 47:4340–4347
- 407 Sacca B, Niemeyer CM (2011) Functionalization of DNA nanostructures with proteins. *Chem Soc*
408 *Rev* 40:5910–5921
- 409 Sacca B, Niemeyer CM (2012) DNA origami: the art of folding DNA. *Angew Chem Int Ed*
410 51:58–66
- 411 Seeman NC (1982) Nucleic acid junctions and lattices. *J Theor Biol* 99:237–247
- 412 Seeman NC (2000) In the nick of space: generalized nucleic acid complementarity and DNA
413 nanotechnology. *Synlett* 11:1536–1548
- 414 Seeman NC (2010) Nanomaterials based on DNA. *Annu Rev Biochem* 79:65–87
- 415 Srinivasan S, Schuster GB (2008) A conjoined thienopyrrole oligomer formed by using DNA as a
416 molecular guide. *Org Lett* 10:3657–3660
- 417 Surana S, Bhat JM, Koushika SP et al (2011) An autonomous DNA nanomachine maps spatio-
418 temporal pH changes in a multicellular living organism. *Nat Commun* 2:340
- 419 Tagawa M, Shohda K, Fujimoto K et al (2011) Stabilization of DNA nanostructures by photo-
420 cross-linking. *Soft Matter* 7:10931–10934
- 421 Totsingan F, Jain V, Bracken WC et al (2010) Conformational heterogeneity in PNA: PNA
422 duplexes. *Macromolecules* 43:2692–2703
- 423 Walsh AS, Yin HF, Erben CM et al (2011) DNA cage delivery to mammalian cells. *ACS Nano*
424 5:5427–5432
- 425 Wei B, Dai M, Yin P (2012) Complex shapes self-assembled from single-stranded DNA tiles.
426 *Nature* 485:623–626
- 427 Winfree E, Liu F, Wenzler LA et al (1998) Design and self-assembly of two-dimensional DNA
428 crystals. *Nature* 394:539–544
- 429 Wojciechowski F, Leumann CJ (2011) Alternative DNA base-pairs: from efforts to expand the
430 genetic code to potential material applications. *Chem Soc Rev* 40:5669–5679
- 431 Yamamoto T, Nakatani M, Narukawa K et al (2011) Antisense drug discovery and development.
432 *Future Med Chem* 3:339–365
- 433 Yang H, Metera KL, Sleiman HF (2010) DNA modified with metal complexes: applications in the
434 construction of higher order metal-DNA nanostructures. *Coord Chem Rev* 254:2403–2415
- 435 Zhang DY, Seelig G (2011) Dynamic DNA nanotechnology using strand-displacement reactions.
436 *Nat Chem* 3:103–113
- 437 Zhang RS, McCullum EO, Chaput JC (2008) Synthesis of two mirror image 4-helix junctions
438 derived from glycerol nucleic acid. *J Am Chem Soc* 130:5846–5847
- 439 Zhu L, Lukeman PS, Canary JW et al (2003) Nylon/DNA: single-stranded DNA with a covalently
440 stitched nylon lining. *J Am Chem Soc* 125:10178–10179